

bond. The pyrimidalization of the nitrogen in **11d** (due to torsion) does not destroy the double-bond character of the P-N bond. The P-N bond length slightly increases by protonation (**10** → **11**) as a consequence of a small charge redistribution.

Finally, the case of methylenephosphorane **12** is quite similar to the preceding one. The compound is better represented as $H_3P=CH_2$ than as $H_3P^+-CH_2$. The centroids corresponding to the double bond are further apart and nearer the phosphorus in **12a** than in **11a** as expected from the corresponding X electronegativities (nitrogen, 3.0; carbon, 2.5).³⁹ Conformation **12d** shows a bent CH_2 and a distorted double bond (the centroid opposed to H_3 is near the phosphorus). The structure corresponds to the description of $Ph_3P=CH_2$ (on the contrary, the arsonium analogue is better represented as $Ph_3As^+-CH_2$).⁴⁰

The most stable structure of methylenephosphorane, **12d**, has been calculated recently by high-level methods. With basis sets like double- ζ augmented with d functions on phosphorus, 6-31G*,⁴² or 3-21G*,³⁵ the optimized geometries are almost identical with those of Table X of the supplementary material (e.g. $d(PO) = 1.667 \pm 0.001 \text{ \AA}$). Better basis sets, 3-21+G*,³⁵ and MP/2-6-31G*⁴² yield slightly different geometries (e.g. $d(PO) = 1.675 \pm 0.002 \text{ \AA}$). The GVB orbitals of **12d** have been discussed by Dixon et al.:⁴¹ they are similar to the LMO's obtained with the

(40) Lloyd, D.; Gosney, I.; Ormiston, R. A. *Chem. Soc. Rev.* **1987**, 16, 45.

(41) Dixon, D. A.; Dunning, T. H.; Eades, R. A.; Gassman, P. G. *J. Am. Chem. Soc.* **1983**, 105, 7011 and references therein.

(42) Yates, B. F.; Bouma, W. J.; Radom, L. *J. Am. Chem. Soc.* **1987**, 109, 2250 and references therein.

Foster and Boys criterion. When the present publication was in press, a theoretical study of methylenephosphorane and related compounds appeared.⁴³

Conclusions

In this paper, we have presented experimental and theoretical evidence of a new class of compounds, the pseudocyclic betaines derived from λ^5 -phosphiniminium salts. Consistent with experimental observations, theory confirms that rotation about the P-N bond results in changes of the nitrogen pyrimidalization.

Registry No. **1**, 109107-00-8; **3a**, 117369-71-8; **3a-C**, 117369-74-1; **3a-D**, 117407-39-3; **3b**, 117369-73-0; **3c**, 117369-72-9; **3c-2CHCl₃**, 117369-75-2; **4d**, 117342-08-2; **6**, 42584-20-3; **7**, 33378-27-7; **8** (isomer1), 82861-54-9; **8** (isomer2), 82857-68-9; **9**, 13840-40-9; **10**, 61559-67-9; **11**, 88392-38-5; **12**, 36429-11-5; MeNCO, 624-83-9; EtNCO, 109-90-0; *n*-PrNCO, 110-78-1; *t*-BuNCO, 1609-86-5.

Supplementary Material Available: Tables of anisotropic thermal parameters, atomic parameters, interatomic distances and angles, and 6-31G* calculated geometries of compounds **9-12d** (52 pages); listings of observed and calculated structure factors (77 pages). Ordering information is given on any current masthead page.

(43) Francl, M. M.; Pellow, R. C.; Allen, L. C. *J. Am. Chem. Soc.* **1988**, 110, 3723.

Communications to the Editor

Sequence-Specific ¹³C NMR Assignment of Nonprotonated Carbons in [d(TAGCGCTA)]₂ Using Proton Detection

Joseph Ashcroft,^{1a} Steven R. LaPlante,^{1b} Philip N. Borer,^{1b} and David Cowburn*^{1a}

The Rockefeller University, 1230 York Avenue
New York, New York 10021
NMR and Data Processing Laboratory
NIH Resource, Syracuse University
Syracuse, New York 13244-1200
Received July 25, 1988

Carbon-13 NMR assignments of protonated carbons can be made by using proton-detected heteronuclear correlation spectroscopy, and this experiment has been applied to DNA oligomers.²⁻⁵ The multibond coupling optimized heteronuclear multispin coherence proton-detected COSY (MC-HMP-COSY) NMR experiment supplies the correlation between ¹³C's and protons that are not directly bonded, but are coupled. This experiment has been applied to vitamin B₁₂,^{6,7} a peptide,⁸ trisaccharides,⁹ and a

Table I. ¹³C Chemical Shifts of Nonprotonated Carbons in [d(TAGCGCTA)]₂

assignment/pathway (proton/carbon)	1-D ¹³ C chemical shift (ppm)	MC-HMP-COSY ¹³ C chemical shift (ppm)
G3(H8 C4)	153.41 ^{a-c}	153.4
G3(H8 C5)	117.49 ^{b,c}	117.8
G5(H8 C4)	153.73 ^{a-c}	153.6
G5(H8 C5)	117.79 ^{b,c}	118.2
C4(H6 C2)	158.95 ^b	159.3
C4(H6 C4)	168.12 ^b	168.1
C6(H6 C2)	158.95 ^b	159.2
C6(H6 C4)	168.25 ^b	168.3
A2(H2 C4)	151.18 ^b	151.3
A2(H8 C5)	120.88 ^b	120.8
A2(H2 C6)	158.30 ^b	158.3
A8(H2 C4)	151.18 ^b	151.25
A8(H8 C5)	120.81 ^b	120.8
A8(H2 C6)	158.11 ^b	158.2
T1(H6 C2)	153.73 ^{a-c}	153.7
T1(Me or H6 C4)	168.83 ^c	169.0
T1(Me C5)	113.87 ^c	114.1
T7(H6 C2)	153.41 ^{a-c}	153.5
T7(Me or H6 C4)	169.37 ^c	169.4
T7(Me C5)	113.57 ^c	113.8

^a Distinction of GC4 and TC2 was ambiguous in the 1D study.^{3,11}

^b Assignments within a carbon class were not clear in the 1D study.^{3,11}

^c Unambiguous assignments made according to MC-HMP-COSY.

polysaccharide with a single repeating monomeric unit,¹⁰ and experimental details are covered in the above cited references.

This communication describes the MC-HMP-COSY experiment applied to the assignments of the nonprotonated carbons

(9) Lerner, L.; Bax, A. *Carbohydr. Res.* **1987**, 166, 35-46.

(10) Byrd, R. A.; Egan, W.; Summers, M. F. *Carbohydr. Res.* **1987**, 166, 47-58.

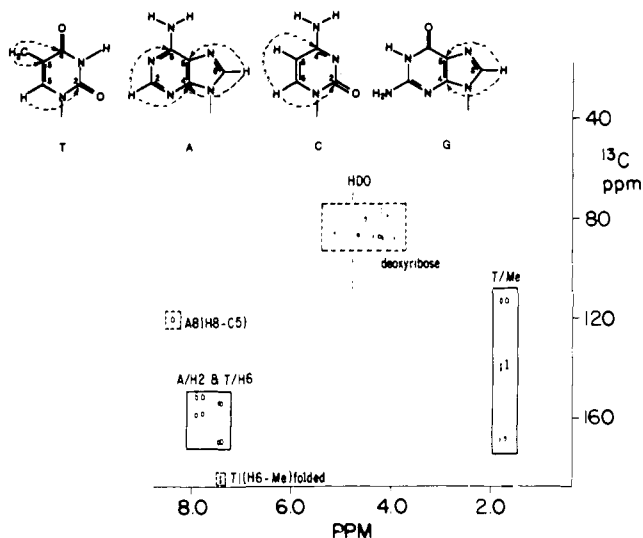


Figure 1. Full MC-HMP-COSY spectrum of $[d(\text{TAGCGCTA})]_2$, synthesized as described in ref 1, 450 A_{260} units in 0.4 mL of 99.96% D_2O with 0.1 M NaCl and 0.1 mM EDTA. The box labeled T/Me contains cross peaks for the thymidine methyl to carbons 4, 5, and 6 and is expanded in Figure 2a. The box labeled A/H2 & T/H6 contains the A2,A8 H2 to carbons 4 and 6, T1,T7 H6 to carbons 2 and 4, and C4,C6 H6 to carbon 4 and is expanded in figure 2b. The substructures at the top illustrate the long-range coupling paths for which corresponding cross peaks were observed here.¹⁸ The pulse sequence used was the following: delay- $90_x(^1\text{H})$ - τ_1 - $90_y(^{13}\text{C})$ - τ_2 - $90_z(^{13}\text{C})$ - τ_3 - $90_x(^{13}\text{C})$ - t_1 - $90_x(^1\text{H})$ - Δ_1 -acquire(^1H) [phase - ϕ]; (phases and timings described below, footnote 12). Data are shown in the absolute value mode.¹⁷ Proton chemical shifts were referenced from the thymidine H6 protons in $[d(\text{TAGCGCTA})]_2$ at 7.39 ppm (relative to 3-(trimethylsilyl)propionic acid-2,2,3,3- D_4 or TSP, see ref 2). The ^{13}C chemical shifts are reported relative to TSP and were obtained by using the indirect referencing method, described previously.^{15,16} The f_2 spectral width was 4201.68 Hz. A total of 4 k complex points were collected in the t_2 domain, resulting in a 1.95-s acquisition period. The evolution delay in the t_1 dimension was incremented in 128 equal steps of 47 μs , resulting in a spectral width of 21 276.59 Hz. A total of 2048 transients were collected and averaged for each t_1 value. The double quantum t_1 dimension was zero-filled to 256 points prior to the last Fourier transform. Areas enclosed by dashed lines have a 1.8 times lower contour level than the remainder of the plotted spectrum. A small residual uncanceled signal from HDO can be seen at 4.67 ppm.

of a DNA oligonucleotide, $[d(\text{TAGCGCTA})]_2$. Chemical shifts of these nonprotonated carbons are of interest, since many have been shown to be sensitive to hydrogen-bonding effects.^{3,11} The complete MC-HMP-COSY spectrum of $[d(\text{TAGCGCTA})]_2$ is shown in Figure 1. The T1 and T7 methyl proton to T1 and T7 $^{13}\text{C}4$, $^{13}\text{C}5$, and $^{13}\text{C}6$ cross peaks are detailed in Figure 2a. The A2 and A8 H2 to C4 and C6 cross peaks are shown in Figure 2b.¹⁸ The ^{13}C chemical shifts of all observed nonprotonated

(11) Borer, P. N.; LaPlante, S. R.; Zanatta, N.; Levy, G. C. *Nucl. Acids Res.* **1988**, *16*, 2323-2332.

(12) Phase cycle used was as follows: α $x, y, -x, -y; -x, -y, x, y; \dots; \beta$ $x, y, -x, -y; x, y, -x, -y; -x, -y, x, y; -x, -y, x, y; \dots; \phi$ $x, y, -x, -y; \dots$. The values of τ_1 , τ_2 , and τ_3 were 2.5, 2.5, and 35 ms. The low pass τ 's were simply chosen to reduce the direct coupling effect in the 100-200-Hz range, without the optimization procedure of ref 13. The delay $\tau_1 + \tau_2 + \tau_3$ was set to approximately $1/3J$, by analogy with the correction for transverse relaxation suggested in ref 14, for the long range coupling of about 8 Hz.

(13) Kogler, H.; Sørensen, O. W.; Bodenhausen, G.; Ernst, R. R. *J. Magn. Reson.* **1983**, *55*, 157-163.

(14) Griffey, R. H.; Redfield, A. G.; Loomis, R. E.; Dahlquist, F. W. *Biochemistry* **1985**, *24*, 817-22.

(15) Bax, A.; Subramanian, S. *J. Magn. Reson.* **1986**, *67*, 565-569.

(16) Live, D. H.; Davis, D. G.; Agosta, W. C.; Cowburn, D. *J. Am. Chem. Soc.* **1984**, *106*, 6104-5.

(17) Data were processed by using a modified UNIX version of Dennis Hare's program FT-NMR. The pulse sequence used does not contain a 180° pulse at the midpoint of the evolution time to eliminate proton offset contributions of f_1 . Post-acquisition processing was used to eliminate the proton offset by implementing a simple algorithm (Ernst, R. R.; Bodenhausen, G.; Wokaun, A. *Principles of Nuclear Magnetic Resonance in One and Two Dimensions*; Oxford University Press: London, 1987; p 337 and 368).

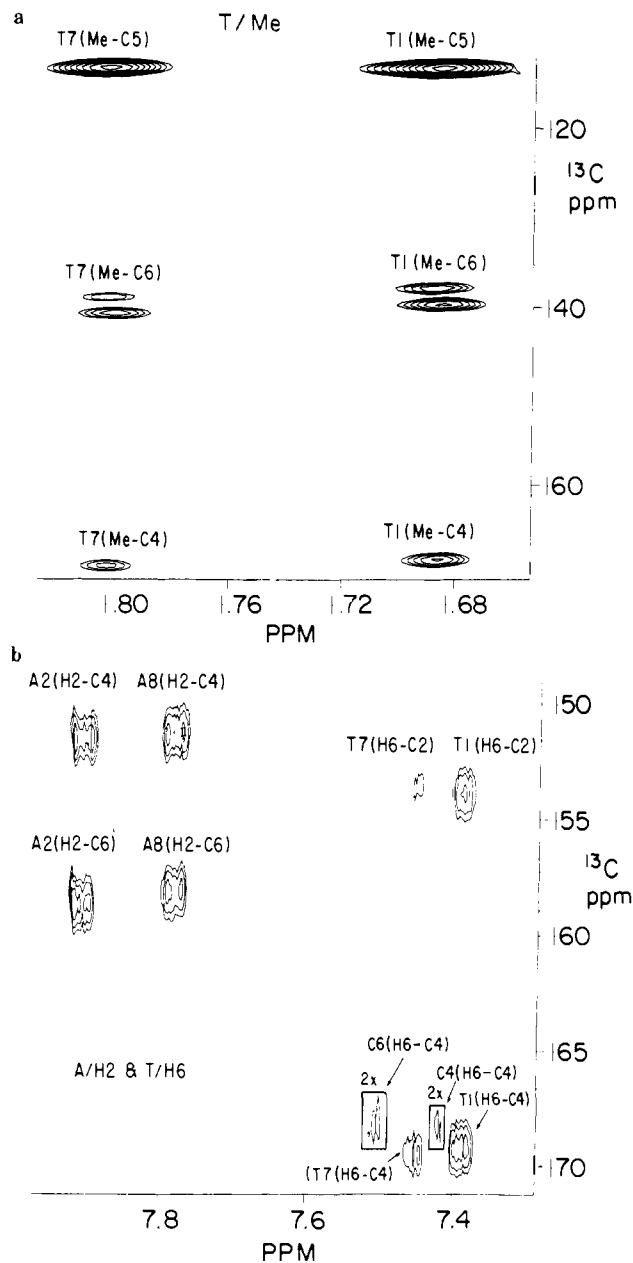


Figure 2. (a) Detail of Figure 1, showing an expansion of the region labeled T/Me. Note the $^1J(^1\text{H}6-^{13}\text{C}6)$ passive coupling splitting the methyl proton- $^{13}\text{C}6$ cross peak in the f_1 dimension, which results from the absence of proton refocussing in the sequence used. (b) Detail of Figure 1, showing an expansion of the region labeled A/H2 & T/H6.

carbon resonances are listed in Table I. The respective columns show the following: (1) the carbon assignment and coupling pathway, (2) the high resolution chemical shifts from a 1D ^{13}C study,³ and (3) the chemical shifts determined in this study. Assignment of GC2 and GC6 could not be made by using MC-HMP-COSY because there is no proton within three bonds of the carbons. The differences in chemical shift which exist are within experimental error (the 2D-MC-HMP COSY experiment has a digital resolution of 1.3 ppm per point).

The data in Table I can be used to contrast the assignments obtained by MC-HMP-COSY with the comparative assignments^{3,11} for the nonprotonated carbons. Not unexpectedly, all of the assignments of carbon class (e.g., GC4, GC5, etc.) agree completely. Some site-specific assignments (G3 C4 vs G5 C4) were ambiguous in the 1D ^{13}C study.^{3,11} MC-HMP-COSY ex-

(18) Guanosine peaks not visible on spectrum shown, see Supplementary Material. Signal-to-noise ratio poor for H8 to Cx cross peaks due to slow exchange with deuterated solvent and possibly unfavorable T_1 's.

periments allowed correlations between site-specific proton assignments³ and ¹³C chemical shifts to be made. These site-specific ¹³C shifts were then compared to the 1D chemical shifts, and the 1D chemical shifts were assigned accordingly. These assignments are marked with superscript italic c in Table I. All of the others are degenerate or within 0.1 ppm of the other, and are correctly assigned according to carbon class.¹⁹

Acknowledgment. Supported by a grant from NSF. Capital equipment at the Rockefeller University supported by grants from NIH, the Keck Foundation, and NSF. D.C. and J.A. acknowledge useful discussions with Dr. John Glushka and Scott Coffin.

Supplementary Material Available: Figures S1 and S2 containing details of the same spectrum as Figure 1 etc., level 2.5 lower than Figure 1, and cross peaks A8(H8-C5), G3(H8-C5), and G5(H8-C5) and G5(H8-C4) and G3(H8-C4), respectively (2 pages). Ordering information is given on any current masthead page.

(19) Since this article was submitted, an experiment for mixed-mode phase-sensitive detection via long-range couplings has been proposed. Bax, A. Marion, D. *J. Magn. Reson.* 1988, 78, 186-188.

Control of Reaction Rates in Vesicular Systems

Iolanda M. Cuccovia,* Maria K. Kawamuro,
Maria A. K. Krutman, and Hernan Chaimovich

*Departamento de Bioquímica, Instituto de Química
Universidade de São Paulo, Caixa Postal 20780
CEP 01498, São Paulo, SP, Brasil*

Received August 17, 1988

Vesicles prepared with synthetic amphiphiles catalyze numerous reactions with high efficiency.¹⁻⁵ Several studies have attempted to separate the kinetic and mechanistic effects of outer and inner surfaces of such vesicles on various chemical reactions.⁵ We here report that a negatively charged substrate (5,5' dithiobis(2-nitrobenzoic acid)) (DTNB) can be selectively incorporated in the inner and/or outer surfaces of vesicles prepared with a positively charged amphiphile (dioctadecyldimethylammonium chloride) (DODAC). Selective incorporation permitted the demonstration of similar interfacial catalysis of the alkaline hydrolysis of DTNB³ by both surfaces. We also demonstrate here, for the first time, that the ratio of the rates of reaction at the inner and outer surfaces can be modulated by changing the composition of the medium.

DTNB (Sigma Chem. Co.) was incorporated in large unilamellar DODAC (Herga Ind. Quim. Brasil) vesicles by injecting a CHCl₃ solution of DODAC (20 mM) into an aqueous solution (70 °C)⁶ containing 5 mM NaCl, 90 mM erythritol, and 0.15 mM DTNB, pH 5.3. This preparation was annealed,⁷ and aliquots were filtered through two columns of Dowex 21K (Cl) (Serva Fine Chemicals)⁸ and eluted with 5.0 mM NaCl/90 mM erythritol. This procedure led to vesicles in which DTNB was adsorbed only

(1) Fendler, J. H. *Membrane Mimetic Chemistry*; Wiley-Interscience: 1982.

(2) Kunitake, T.; Okahata, Y.; Ando, R.; Shinkai, S.; Hirakawa, S. *J. Am. Chem. Soc.* 1980, 102, 7877.

(3) Fendler, J. H.; Hinze, W. L. *J. Am. Chem. Soc.* 1981, 103, 5439.

(4) Chaimovich, H.; Bonilha, J. B. S.; Zanette, D.; Cuccovia, I. M. In *Surfactants in Solution*; Mittal and Lindmann, Eds.; Plenum Press: New York, 1984; Vol. 3, p 1121.

(5) (a) Moss, R. A.; Schreck, P. *J. Am. Chem. Soc.* 1985, 107, 6634. (b) Moss, R. A.; Battacharya, S.; Scrimin, P.; Swarup, S. *J. Am. Chem. Soc.* 1987, 109, 5740. (c) Moss, R. A.; Swarup, S.; Zhang, H. *J. Am. Chem. Soc.* 1988, 110, 2914.

(6) Ribeiro, A. M. C.; Chaimovich, H. *Biochim. Biophys. Acta* 1983, 733, 172.

(7) (a) Without annealing^{7b} the endovesicular rate constants were faster and not reproducible. (b) Elamrani, K.; Blume, A. *Biochim. Biophys. Acta* 1983, 727, 22.

(8) Tricot, Y. M.; Furlong, D. N.; Sasse, W. H. F.; Daivis, P.; Snook, I.; Van Megen, W. *J. Colloid Interface Sci.* 1984, 97, 380.

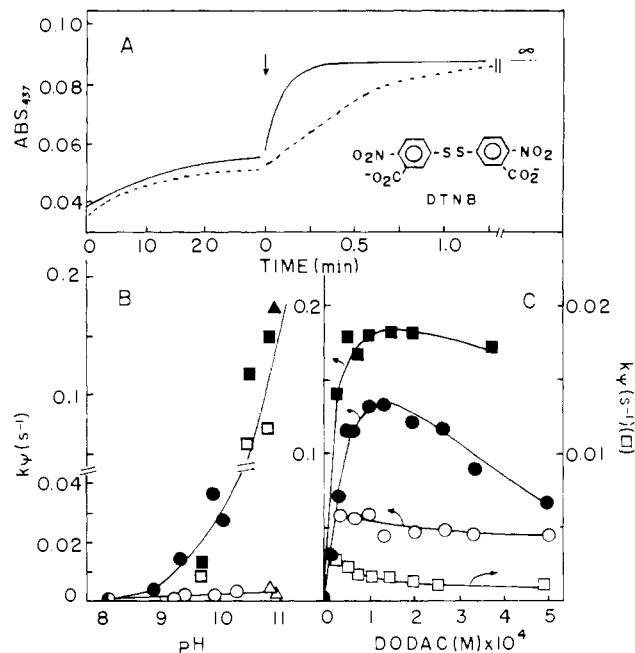


Figure 1. A. Chloride and bromide effects on the endo- and exovesicular hydrolysis of DTNB. [DODAC] = 5.3×10^{-5} M, [DTNB] (endovesicular, analytical) = 2×10^{-6} M. The arrow indicates the addition of external DTNB 2×10^{-6} M final concentration): (—) NaOH 1 mM, NaCl 4 mM, pH 10.9; (---) NaOH 1 mM, NaBr 4 mM, pH 10.8. B. pH effects on the rate of the endo- and exovesicular hydrolysis of DTNB: [DTNB] (endovesicular, analytical) = [DTNB] (exovesicular) = 2×10^{-6} M; [DODAC] = 4×10^{-5} M. NaCl was added to maintain the total anionic concentration at 5 mM. Full points indicate exovesicular, and open points refer to the endovesicular reactions, respectively: (●, ○), borate buffer, 5 mM; (■, □), triethylamine-HCl buffer, 5 mM at pH 9.7, 3.3 mM at pH 10.5, and 10 mM at pH 10.9; (▲, △), NaOH 1 mM. C. Effect of DODAC concentration on the rate of endo- and exovesicular hydrolysis of DTNB. [DTNB] (endovesicular, analytical) = [DTNB] (exovesicular) = 2×10^{-6} M. NaCl was added to maintain the total ionic concentration at 5 mM. Full points indicate exovesicular, and open points refer to endovesicular reactions, respectively: (●, ○) triethylamine-HCl buffer, 3.3 mM, pH 10.5; (■, □) NaOH 1 mM, pH 10.91.

to the internal surface.⁹ DTNB hydrolysis (30 °C) was followed (437 nm)³ in a Beckmann DU7 spectrophotometer.

The endovesicular reaction was started by adding aliquots of the (column-eluted) vesicle pool (0.6 mM DODAC¹⁰ and 0.03 mM DTNB) to a solution at the desired pH with osmolarity and ionic strength controlled with erythritol and NaCl, respectively. After the complete reaction $2 \mu\text{L}$ of a 1 mM aqueous solution of DTNB was added to the same cuvette. The ensuing absorbance increase was attributed to reaction at the external vesicular surface since (a) the rate constant¹¹ for this exovesicular process was similar to one obtained previously³ and (b) DTNB does not penetrate the bilayer under our conditions.⁹ Figure 1A shows a typical endo- and exovesicular hydrolysis of DTNB. Using the same procedure, kinetic data were obtained under several conditions (Figure 1B, Table I). In the absence of buffer and at high pH, the exovesicular reaction was 100 times faster than the endo process (Figure 1 (parts B and C), Table I). However, with borate or triethylamine buffers, the endo- and exovesicular rate constants were of the same order of magnitude (Table I, Figure 1 (parts B and C)). The maximum rate enhancement in the presence of vesicles, with respect to the uncatalyzed reaction, was 200-fold (Table I). The (low) rate observed for endovesicular

(9) Twenty hours after vesicle preparation the rate constant for the endovesicular reaction was identical with that obtained immediately after annealing indicating that DTNB did not leak out of the vesicles.

(10) Stelmo, M.; Chaimovich, H.; Cuccovia, I. M. *J. Colloid Interface Sci.* 1987, 117, 200.

(11) The rate constants were obtained from a computer-fit of a first-order process. After passage through ion-exchange columns the kinetics revealed approximately 10% of exovesicular reaction in the absence of added buffer.